

Time Dependence of the Echelle Modes Sensitivity before the STIS Repair

Alessandra Aloisi
September 30, 2011

ABSTRACT An analysis of all the monitoring observations taken for some representative echelle prime modes during a period (September 1997 - May 2004) covering STIS on-orbit operations before the STIS Side-2 failure, is presented in this report. This analysis demonstrates that before the STIS repair the echelle modes had a time dependence of their sensitivity that followed closely the trends observed in G140L and G230L by Stys et al. (2004) at corresponding wavelengths. A correction for a temperature- and time-dependent sensitivity of all echelle modes based on the correction applied to the first-order modes, was implemented into the STIS calibration pipeline as of April 2005.

Introduction

Programs to monitor the sensitivity of the STIS detectors in spectroscopic modes with external flux standard stars started during SMOV2 immediately following installation of STIS on HST back in February 1997. This monitoring continued periodically throughout STIS operations until failure of the Side-2 electronics in August 2004, and resumed after completion of SMOV4 following the STIS repair during SM4 in May 2009.

Back at the beginning of STIS on-orbit operations, a weekly monitoring of the first-order L modes was immediately started during SMOV2, while a periodic but less frequent monitoring of a representative set of first-order M modes and echelle modes started in September 1997 as part of Cycle 7 STIS Calibration Program. The frequencies of these observations varied depending on the detectors and the modes involved, with the most frequently monitored modes being the MAMA first-order L modes.

For an analysis of the sensitivity monitoring observations of the STIS first-order modes up to the Side-2 failure, please refer to the previous STIS Instrument Science Reports (ISRs) published by Walborn & Bohlin (1998), Bohlin (1999), Smith et al. (2000),

Stys & Walborn (2001), and Stys et al. (2004). All these reports established clear evidence for wavelength-dependent variations of the UV throughput over time at rates that were in some periods as high as 3% and 1-2% per year in the FUV and NUV, respectively. In this report, we provide for the first time a complete analysis of the sensitivity monitoring observations of the STIS echelle medium- and high-resolution modes covering the whole period of Side-1 and Side-2 operations before the STIS repair (1997-2004). Results from the STIS sensitivity monitoring program after the STIS repair will be presented in a forthcoming ISR.

Observations

The relatively bright ($V = 10.52$ mag) spectrophotometric standard star BD+28°4211 was monitored with each STIS echelle grating about every 6 months in order to detect changes in sensitivity due to contamination or other causes. Only one prime mode per grating was monitored with the exception of E230M, for which both available prime modes were considered covering the whole wavelength range of the grating sensitivity. In particular, the monitored echelle prime modes are E140H 1416 Å, E140M 1425 Å, E230H 2263 Å, E230M 1978 Å and 2707 Å.

All echelle monitoring observations (see Table 1) were obtained as part of a similar calibration program executed in each cycle starting from Cycle 7 and ending with Cycle 12 (programs 7673, 8424, 8857, 8919, 9628, and 10033). The period covered by these observations goes from December 1997 to May 2004. The data were acquired with the $0.2'' \times 0.2''$ aperture following standard peak-up target acquisition. The monthly offsetting (MO) of the Mode Select Mechanism, which normally occurs for MAMA spectra, was disabled for these observations (i.e., a zero MO was used) in order to minimize variations due to the spatial displacement of the spectra on the detector.

In addition to the monitoring data mentioned above, some other early observations of the standard star BD+28°4211 taken with a zero MO and a $0.2'' \times 0.2''$ aperture in some of the monitored echelle modes, were also considered. These observations were obtained as part of the SMOV2 program 7096 (September 1997) and the Cycle 7 calibration program 7657 (December 1998). These additional observations (see Table 1) were executed to determine the baseline sensitivity of the echelle modes rather than to monitor the time dependence.

Analysis

All the data were calibrated with the STSDAS version of the CALSTIS pipeline and the most up-to-date reference files as of February 2005. For our analysis we considered the observed net count rate as a function of wavelength as obtained from the standard one-dimensional extraction (x1d files) of each order within each spectrum.

An analysis procedure similar to the one performed on the monitoring data of the STIS first-order modes was adopted (see Stys et al. 2004 and references therein). For the echelle data, however, the net count rate within each order was considered instead of the

net count rate within each 50 Å wavelength bin. In addition, the net counts were first rectified in order to properly handle effects related to the echelle blaze function during the comparison at different epochs. Also, no attempt was made to fold into the analysis the sensitivity changes with instrumental temperature as done instead by Stys et al. (2004) for the first-order modes. This is because the observations considered in this report have instrumental temperatures in the range $\sim 35\text{-}40^\circ\text{C}$ (i.e., well around the reference temperature of 36°C) as inferred from the charge amplifier temperature keywords OM1CAT and OM2CAT for the FUV and NUV MAMAs, respectively. Such temperatures typically contribute to much less than $\sim 1\%$ in sensitivity changes and only in the FUV spectral region (no significant dependence of sensitivity on temperature was observed for the NUV MAMA first-order modes). The only exception to this are the very early SMOV2 observations from program 7096 (flagged with an asterisk in Table 1), with temperatures significantly lower than for other subsequent observations. The possibility of strong thermal effects (not only on the sensitivity), in addition to the possibility of other uncertainties related to these being some of the very first observations taken in a certain echelle mode, led to exclude these observations from our analysis.

In the case of STIS the echelle blaze function of a given order varies with the location of that order on the detector (e.g., due to the MSM monthly offsets) and with the passage of time on orbit (see, e.g., Bowers & Lindler 2002, and Aloisi 2007). In particular, both factors contribute to a shift of the blaze function compared to the wavelength scale ¹. All the echelle monitoring data considered in this report have zero MO. This ensures that the “spatial” component of the blaze shift is negligible for our purposes. On the other hand, the long period spanned by the data introduces a “temporal” component that needs to be properly taken into account. This is why the net counts need to be rectified before proceeding to calculate the ratio between the net counts in an observation at a certain epoch and the net counts in the first dataset.

¹The shift of the echelle blaze function (BSHIFT) varies linearly with the position of the spectra on the detector and with the passage of time on orbit. This shift is currently corrected within the pipeline, but this was not the case at the time of the analysis of the data used in this report. The blaze shift correction works as follows. During the processing of an echelle dataset, the following parameters are first determined from the x1d file: wavelength (OBSW), cross-dispersion position (OBSY), and dispersion (DISP in Å/pix) of the reference spectral order REFORD at pixel $x=512$. The shift in pixels is then computed using the formula:

$$\text{BSHIFT} = \text{BSHIFT_VS_X} * \Delta x + \text{BSHIFT_VS_Y} * \Delta y + \text{BSHIFT_VS_T} * \Delta t + \text{BSHIFT_OFFSET} ,$$

where $\Delta x = (\text{REFWAV} - \text{OBSW}) / \text{DISP}$, $\Delta y = \text{OBSY} - \text{REFY}$, $\Delta t = \text{OBSDATE} - \text{REFMJD}$, and OBSDATE is the Modified Julian Day (MJD) of the observation. REFWAV and REFY are, respectively, the wavelength and cross-dispersion position of the reference spectral order REFORD at pixel $x=512$, and REFMJD is the MJD of the observations used to infer the sensitivity of the echelle mode. An average of these parameters is taken if more than one reference observation is available for a certain mode. The linear coefficients BSHIFT_VS_X and BSHIFT_VS_Y relative to the spatial component of the blaze shift, vary with the grating used. The linear coefficients BSHIFT_VS_T and BSHIFT_OFFSET referring to the temporal component of the blaze shift, vary instead with the grating, order, and side of STIS operations (Side 1 or Side 2 before failure; a characterization of Side 2 after STIS repair still remains to be done). See Aloisi & Bostroem (2012, in preparation) for more details.

The rectification was performed with the following procedure. The spectral continuum defined by the vector of the net count rate was fitted with a third or fourth order polynomial, the fit representing the blaze function specific to the considered observation. The net count rate was then divided by a version of the fit normalized to the fit maximum. The latter normalization is necessary in order not to annul the effects of time-dependent sensitivity (TDS) on our data. Table 2 reports the orders within each echelle prime mode here analyzed, where this rectification procedure failed because of a bad fit of the blaze function, e.g., due to strong contamination by absorption lines or edge effects.

For each order the sum of the “rectified” net counts over a certain wavelength range (approximately the central 600 over 1024 pixels of the order, i.e., in a region where the blaze function is not supposed to vary drastically with wavelength) was then divided by the sum of the “rectified” net counts over the same wavelength region in the first dataset used as reference. Finally, this ratio was normalized to properly take into account the TDS correction of the first dataset as inferred from the trend of the first-order modes. The relative sensitivities obtained in this way (red asterisks) are plotted as a function of time in Figures 1 to 5 for, respectively, all the echelle prime modes considered in this analysis. Each order is displayed in a separate panel of each figure. Please refer to Table 2 for a list of orders where this kind of analysis may be moot due to a bad fit of the blaze function.

In Figures 1-5 we also show the TDS trends obtained for the first-order modes by Stys et al. (2004), in particular G140L (1150-1700 Å) for the FUV and G230L (1600-3100 Å) for the NUV spectral regions (black solid lines). The direct comparison of the red asterisks with the black solid lines clearly indicates that the TDS trend of the echelle modes is quite similar to that observed for the first-order modes. This suggests that to first order the changes in sensitivity described in this report are not related to particular gratings. These changes do not appear to be related to changes in the detectors either, as a similar TDS behavior is seen for the first-order modes G230L (NUV MAMA) and G230LB (CCD) in Stys et al. (2004). The changes are more likely associated with contamination or changes within the STIS optics or more in general the HST optics.

Many uncertainties affect a proper determination of the TDS trend from the echelle data, in particular (1) a much coarser sampling over time compared to the first-order modes, (2) a more likely loss of flux from one observation to the other due to the much smaller aperture used ($0.2'' \times 0.2''$ for the echelle modes versus $52'' \times 2''$ for the first-order modes), (3) a larger scatter in the results due to the blaze function (shape and shift) which introduces additional differences in the net count rate at a certain wavelength independently of TDS effects, and (4) uncertainties in the blaze function fit, especially in regions heavily contaminated by absorption lines. For all the above mentioned reasons, no attempt was made to infer a TDS trend for the echelle modes directly from the analysis presented in this report, and the temperature- and time-dependent sensitivity correction applied to the first-order modes was also adopted for the echelle data. The black asterisks in Figures 1-5 represent the ratios of the echelle net count rate after the

application of such a correction to the observations here analyzed.

TDS Correction Applied in the Pipeline

Corrections for the temperature and time dependency of the sensitivity of all echelle data were incorporated into the STScI data-reduction pipeline as of April 4, 2005 with the delivery of new TDSTAB reference files that extend these corrections from the first-order modes only to also the echelle modes.

In light of this delivery, the uncertainties associated to the absolute sensitivity of the echelle modes are reduced from about 15-20% to less than a few % (see Figures 1-5).

Acknowledgements

We thank Paul Goudfrooij, Ralph Bohlin, Phil Hodge, and Charles Proffitt for helpful discussion. We thank James Davies, Rosa Diaz-Miller and Jessica Kim Quijano for technical support in the implementation of the TDS for the echelle modes and Ralph Bohlin for a prompt review of this document before publication.

References

- Aloisi, A. 2006, 2005 HST Calibration Workshop, eds. A. Koekemoer, P. Goudfrooij, & L. Dressel (Baltimore: STScI), 190
- Aloisi, A., & Bostroem, A. 2012, STIS ISR, “Blaze-Shift Correction for STIS Echelle Data”, in preparation
- Aloisi, A., Bohlin, R., & Kim Quijano, J. 2007, STIS ISR 2007-01, “New On-Orbit Sensitivity Calibration for All STIS Echelle Modes”
- Bohlin, R. 1999, STIS ISR 1999-07, “Changes in Sensitivity of the Low-Dispersion Modes”
- Bowers, C., & Lindler, D. 2003, 2002 HST Calibration Workshop, eds. S. Arribas, A. Koekemoer, & B. Whitmore (Baltimore: STScI), 127
- Smith, E., Stys, D. J., Walborn, N. R., & Bohlin, R. 2000, STIS ISR 2000-03, “Sensitivity Monitor Report for the STIS First-Order Modes - II”
- Stys, D. J., Bohlin, R. C., & Goudfrooij, P. 2004, STIS ISR 2004-04, “Time-Dependent Sensitivity of the CCD and MAMA First-Order Modes”
- Stys, D. J., & Walborn, N. R. 2001, STIS ISR 2001-01, “Sensitivity Monitor Report for the STIS First-Order Modes - III”
- Walborn, N. R., & Bohlin, R. 1998, STIS ISR 1998-27, “Sensitivity Monitor Report for the STIS First-Order Modes”

Table 1. Observations of the standard star BD+28°4211 used to monitor the sensitivity of the echelle gratings.

Grating	Central wavelength	Proposal ID	Dataset	Observation date	Exposure time (s)		
E140H	1416	7673	O45930010	1997-12-30	935		
			O45931030	1998-05-20	994		
			O45932030	1998-09-13	994		
			O45933030	1999-01-15	994		
			O45934030	1999-05-22	994		
		8424	O5JJ22030	1999-11-10	1040		
			O5JJ23030	2000-05-15	1040		
		8857	O69S19030	2000-11-09	1040		
			O69S20030	2001-08-26	1040		
		8919	O6I819030	2001-11-28	1040		
			O6I820030	2002-05-27	1040		
		9628	O8IA12030	2002-11-01	1040		
			O8IA13030	2003-05-03	1040		
		10033	O8V560030	2003-12-23	1040		
			O8V561030	2004-05-10	1040		
		E140M	1425	7096	O3ZX02X5Q*	1997-09-19	1779
				7673	O45930030	1997-12-30	350
O45931020	1998-05-20				350		
O45932020	1998-09-13				350		
O45933020	1999-01-15				350		
O45934020	1999-05-22				350		
8424	O5JJ22020			1999-11-10	350		
	O5JJ23020			2000-05-15	350		
8857	O69S19020			2000-11-09	350		
	O69S20020			2001-08-26	350		
8919	O6I819020			2001-11-28	350		
	O6I820020			2002-05-27	350		
9628	O8IA12020			2002-11-01	350		
	O8IA13020			2003-05-03	350		
10033	O8V560020			2003-12-23	350		
	O8V561020			2004-05-10	350		
E230H	2263			7673	O45930020	1997-12-30	1617
		O45931010	1998-05-20		1618		
		O45932010	1998-09-13		1618		
		O45933010	1999-01-15		1618		
		O45934010	1999-05-22		1618		
		8424	O5JJ22010	1999-11-10	1455		
			O5JJ23010	2000-05-15	1455		
		8857	O69S19010	2000-11-09	1455		
			O69S20010	2001-08-26	1476		
		8919	O6I819010	2001-11-28	1476		
			O6I820010	2002-05-27	1476		

Table 1. (cont'd)

Grating	Central wavelength	Proposal ID	Dataset	Observation date	Exposure time (s)
		9628	O8IA12010	2002-11-01	1476
			O8IA13010	2003-05-03	1476
		10033	O8V560010	2003-12-23	1476
			O8V561010	2004-05-10	1652
E230M	1978	7096	O3ZX02XAQ*	1997-09-19	1136
		7657	O4DD15020	1998-12-03	720
		7673	O45930040	1997-12-30	430
			O45931040	1998-05-20	516
			O45932040	1998-09-13	516
			O45933040	1999-01-15	516
			O45934040	1999-05-22	516
		8424	O5JJ22040	1999-11-10	516
			O5JJ23040	2000-05-15	516
		8857	O69S19040	2000-11-09	516
			O69S20040	2001-08-26	516
		8919	O6I819040	2001-11-28	516
			O6I820040	2002-05-27	516
		9628	O8IA12040	2002-11-01	516
			O8IA13040	2003-05-03	516
		10033	O8V560040	2003-12-23	516
			O8V561040	2004-05-10	516
E230M	2707	7096	O3ZX02XEQ*	1997-09-19	1085
			O3ZX02XGQ*	1997-09-19	618
		7657	O4DD15030	1998-12-03	720
		7673	O45930050	1997-12-30	365
			O45931050	1998-05-20	438
			O45932050	1998-09-13	438
			O45933050	1999-01-15	438
			O45934050	1999-05-22	438
		8424	O5JJ22050	1999-11-10	438
			O5JJ23050	2000-05-15	438
		8857	O69S19050	2000-11-09	438
			O69S20050	2001-08-26	438
		8919	O6I819050	2001-11-28	438
			O6I820050	2002-05-27	438
		9628	O8IA12050	2002-11-01	438
			O8IA13050	2003-05-03	438
		10033	O8V560050	2003-12-23	438
			O8V561050	2004-05-10	438

Table 2. Orders where the blaze function was not properly fitted.

Grating	Central wavelength	Orders
E140H	1416	284, 290
E140M	1425	86, 93, 96, 107, 111, 125
E230H	2263	...
E230M	1978	87, 88, 89
E230M	2707	...

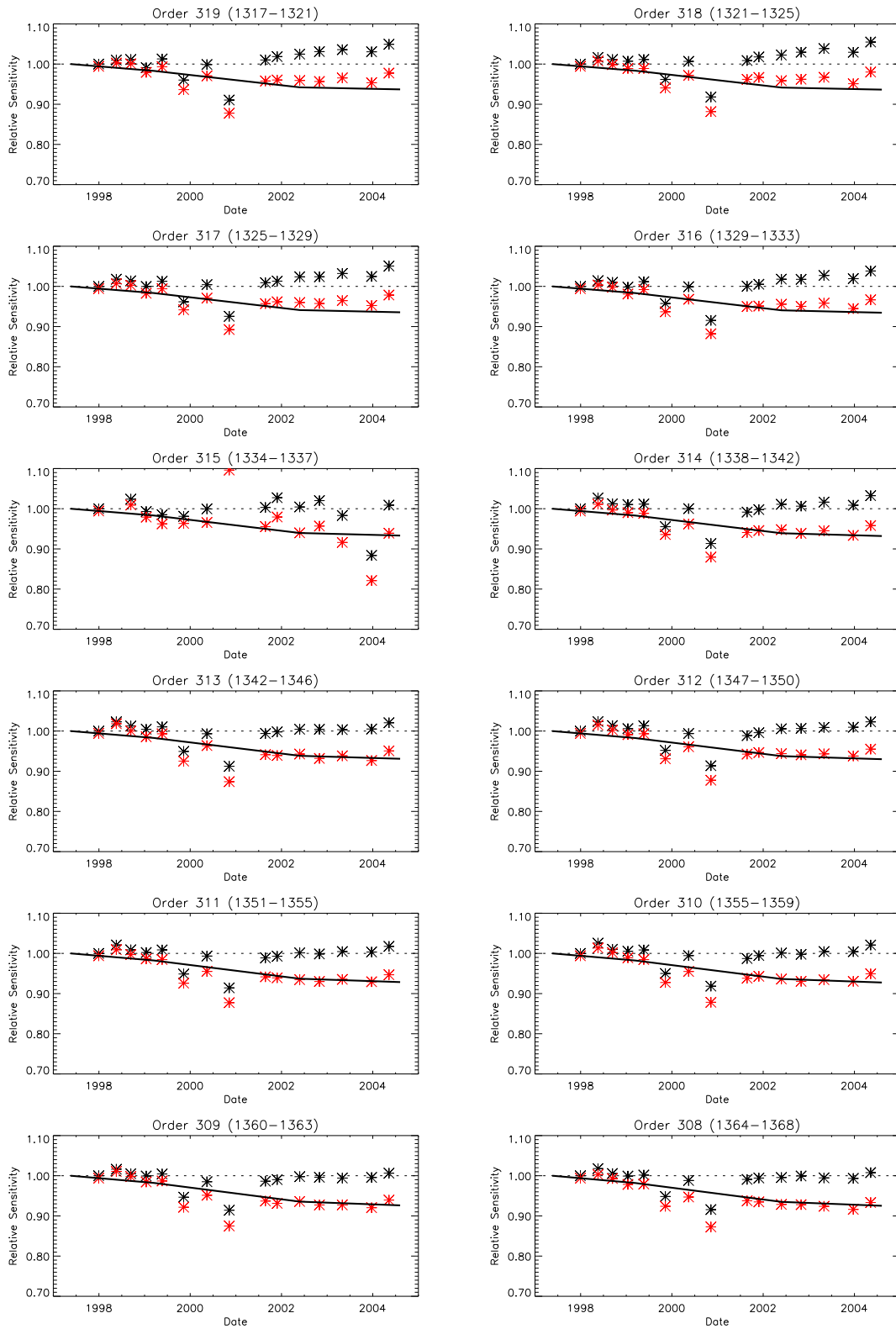


Figure 1. E140H at the central wavelength 1416 Å (~ 1315-1515 Å).

Instrument Science Report STIS 2011-04

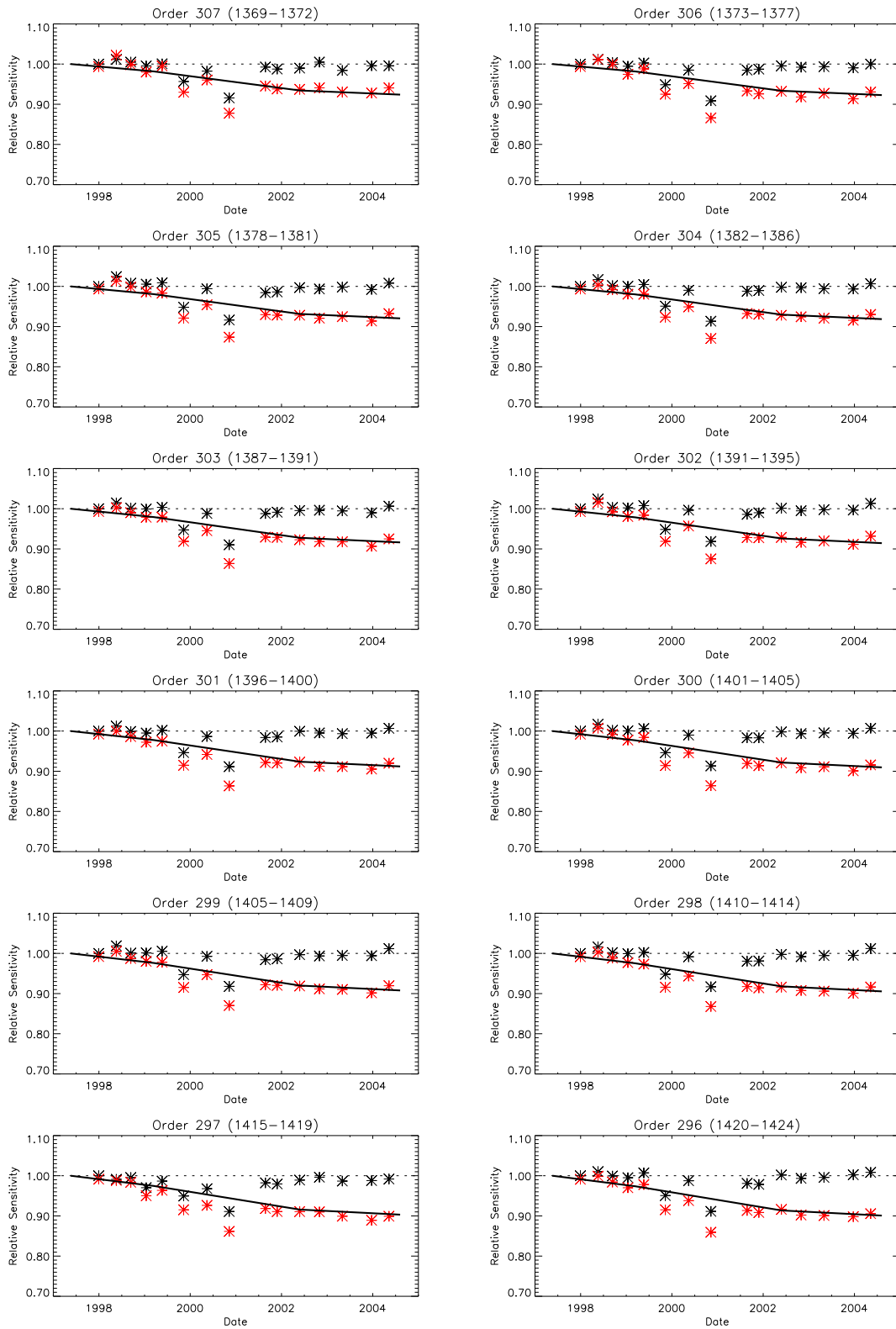


Figure 1. (cont'd)

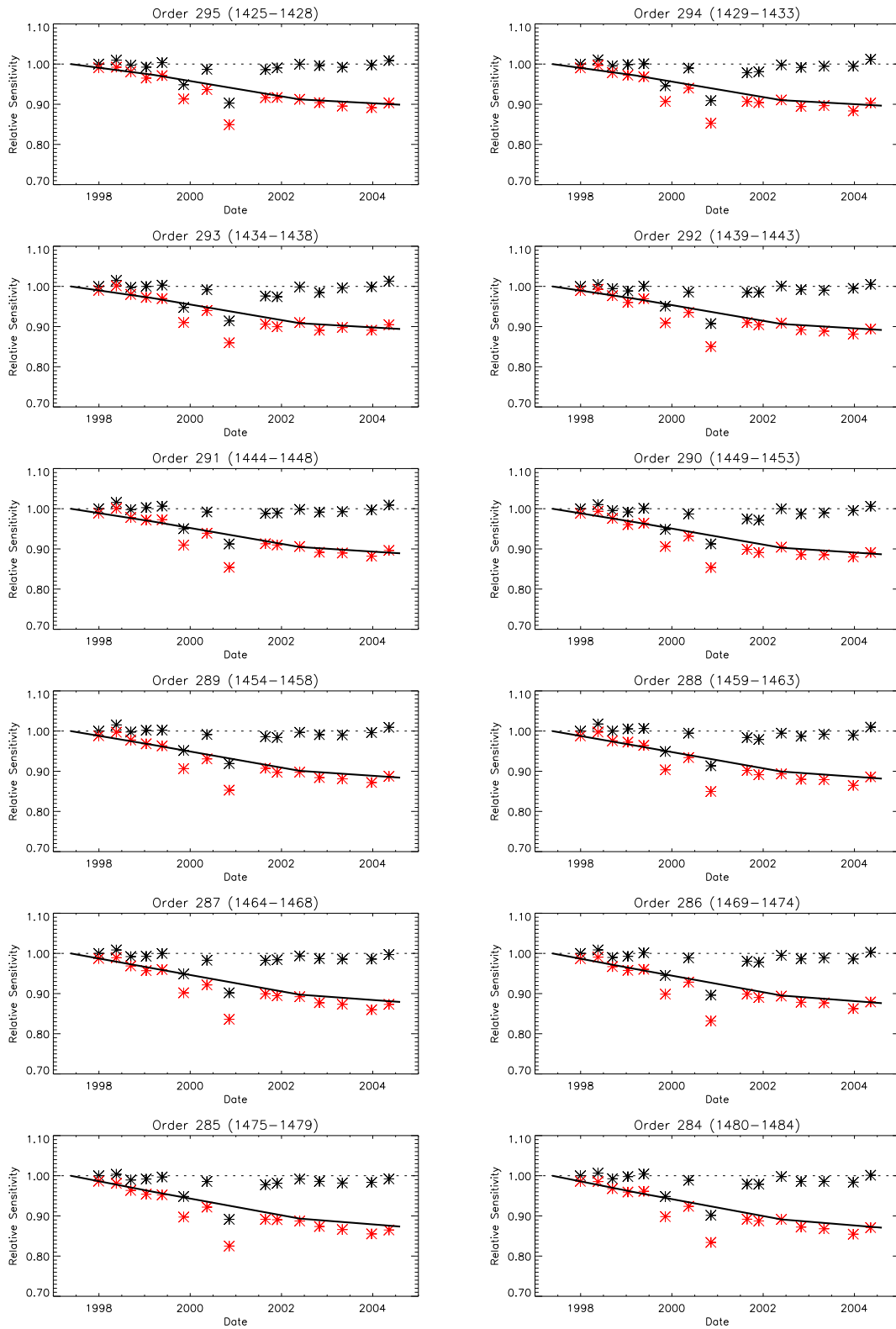


Figure 1. (cont'd)

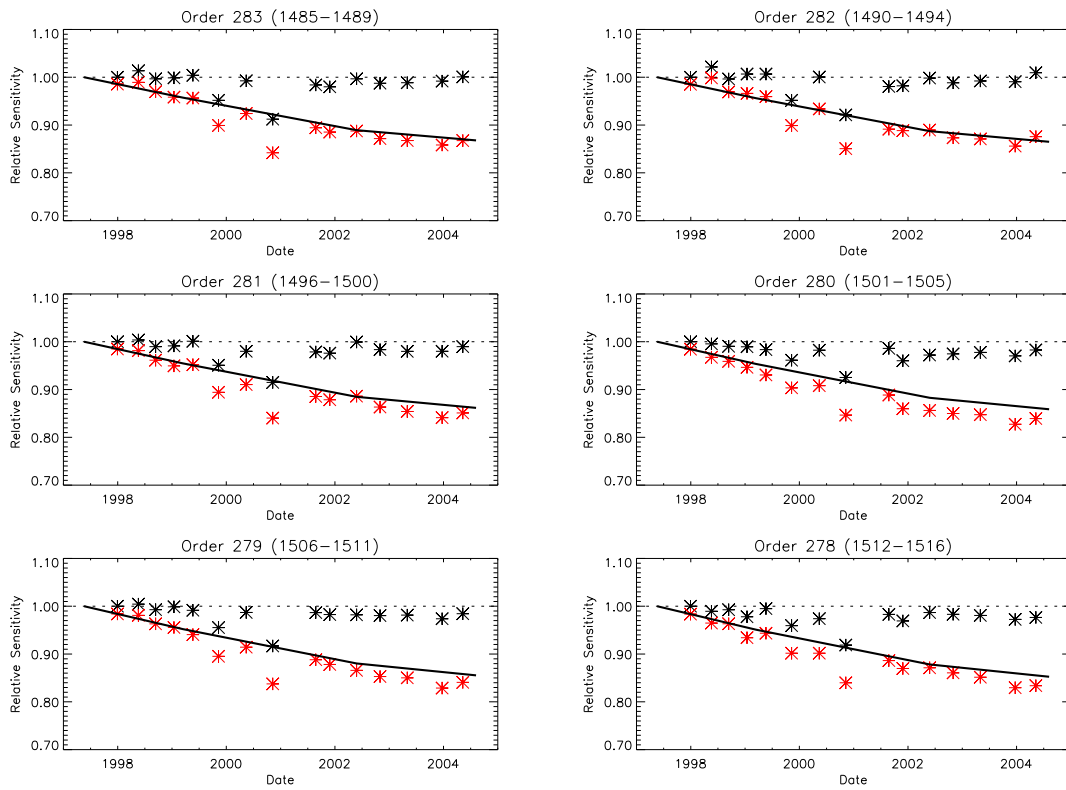


Figure 1. (cont'd)

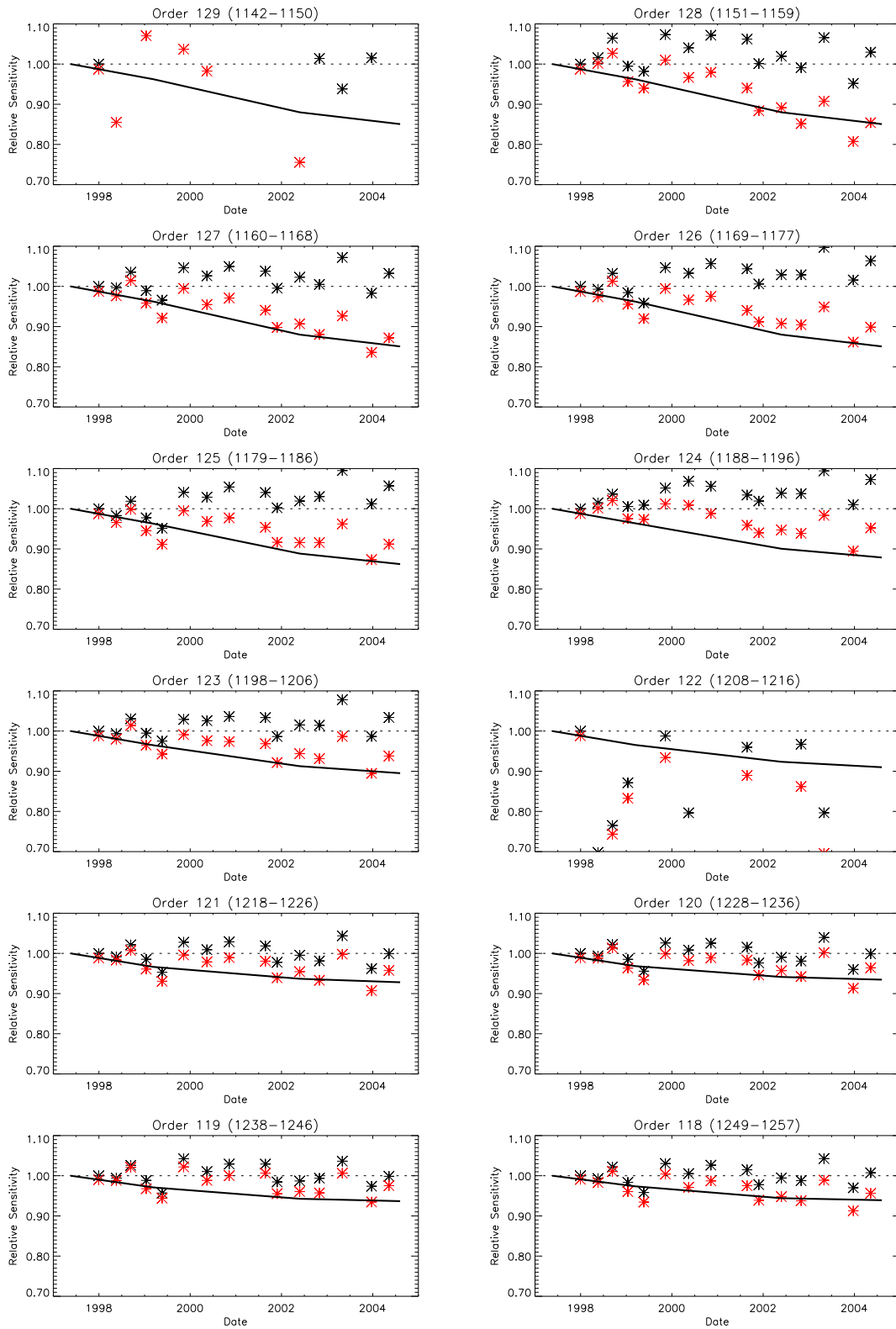


Figure 2. E140M at the central wavelength 1425 Å (~ 1120-1710 Å).

Instrument Science Report STIS 2011-04

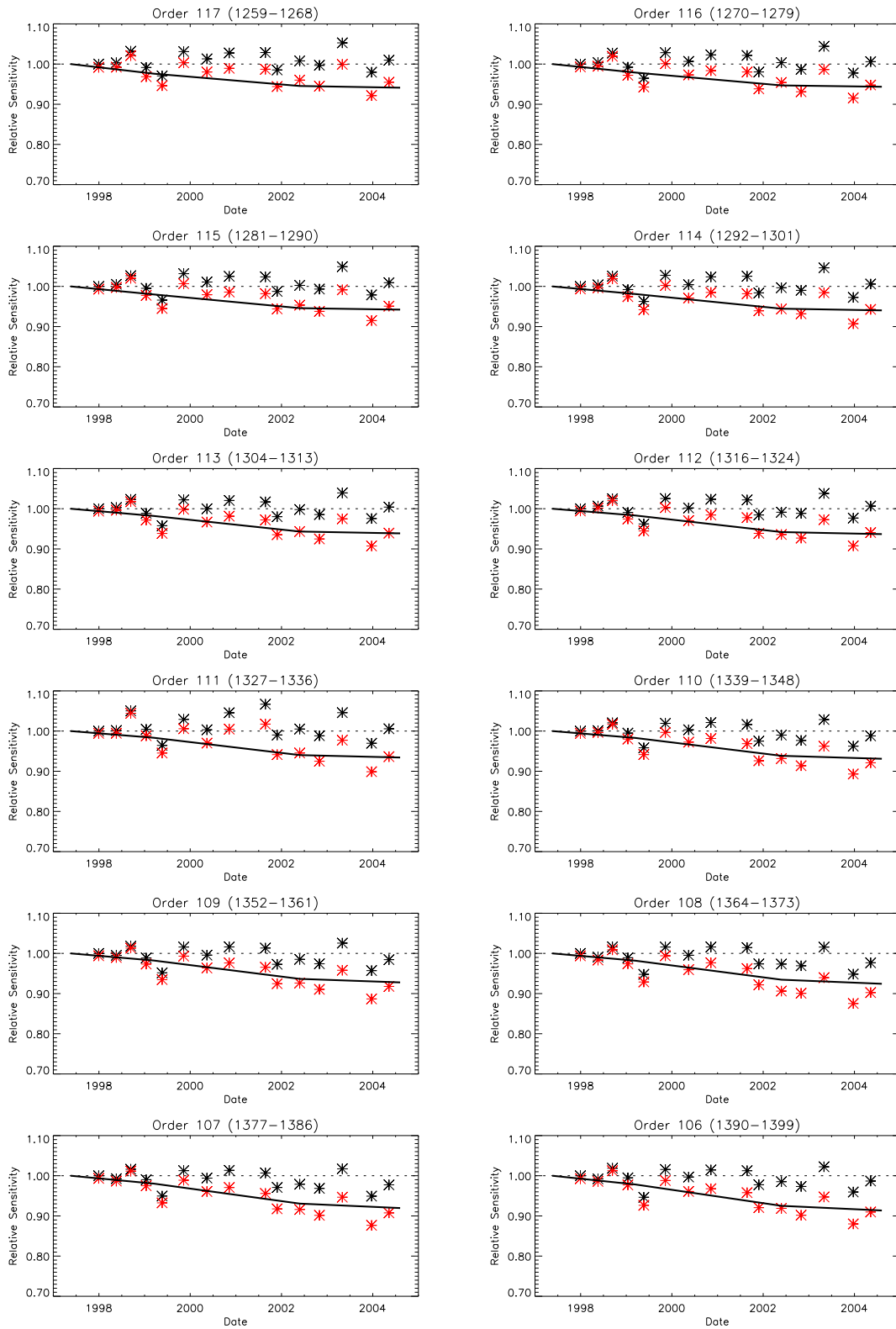


Figure 2. (cont'd)

Instrument Science Report STIS 2011-04

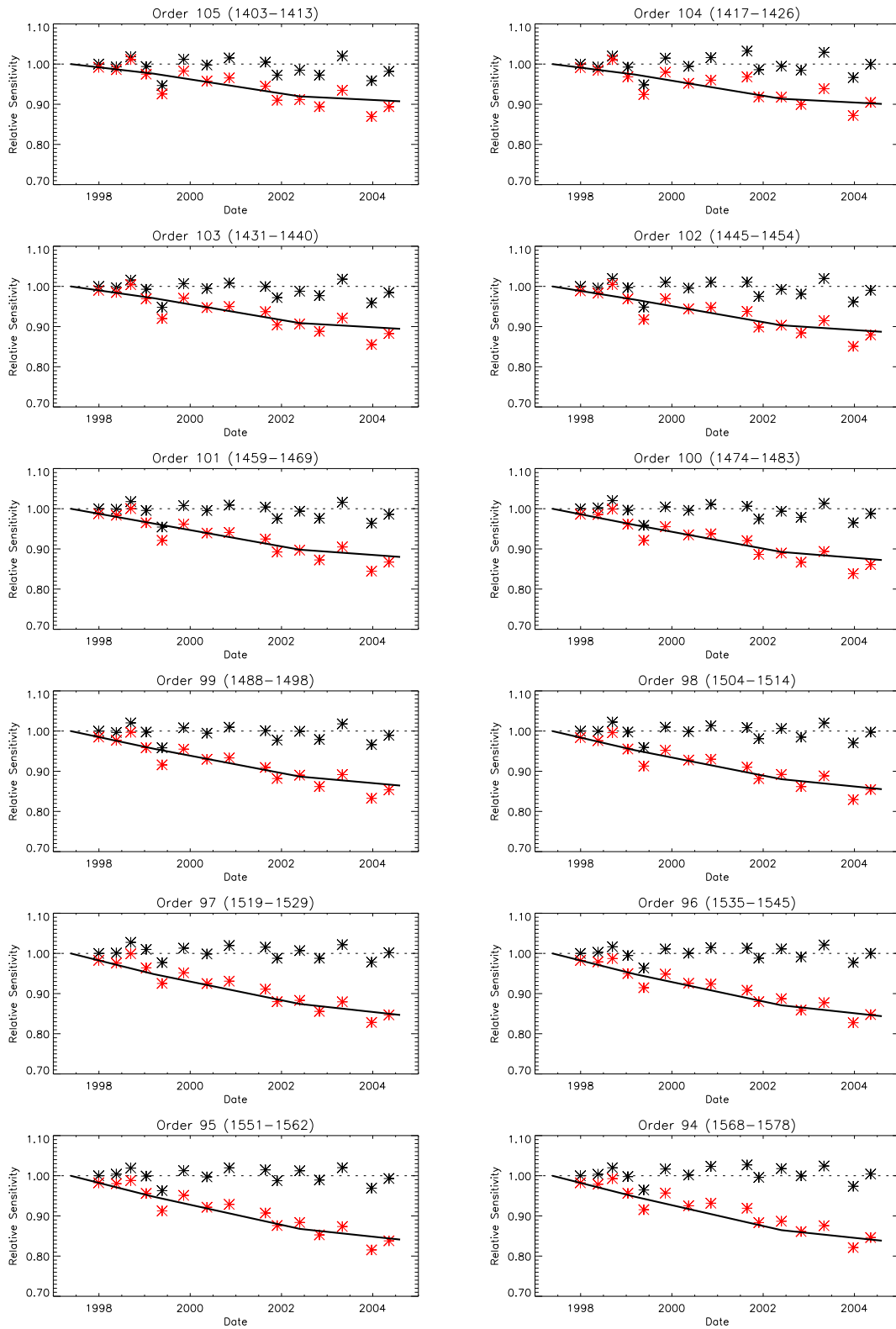


Figure 2. (cont'd)

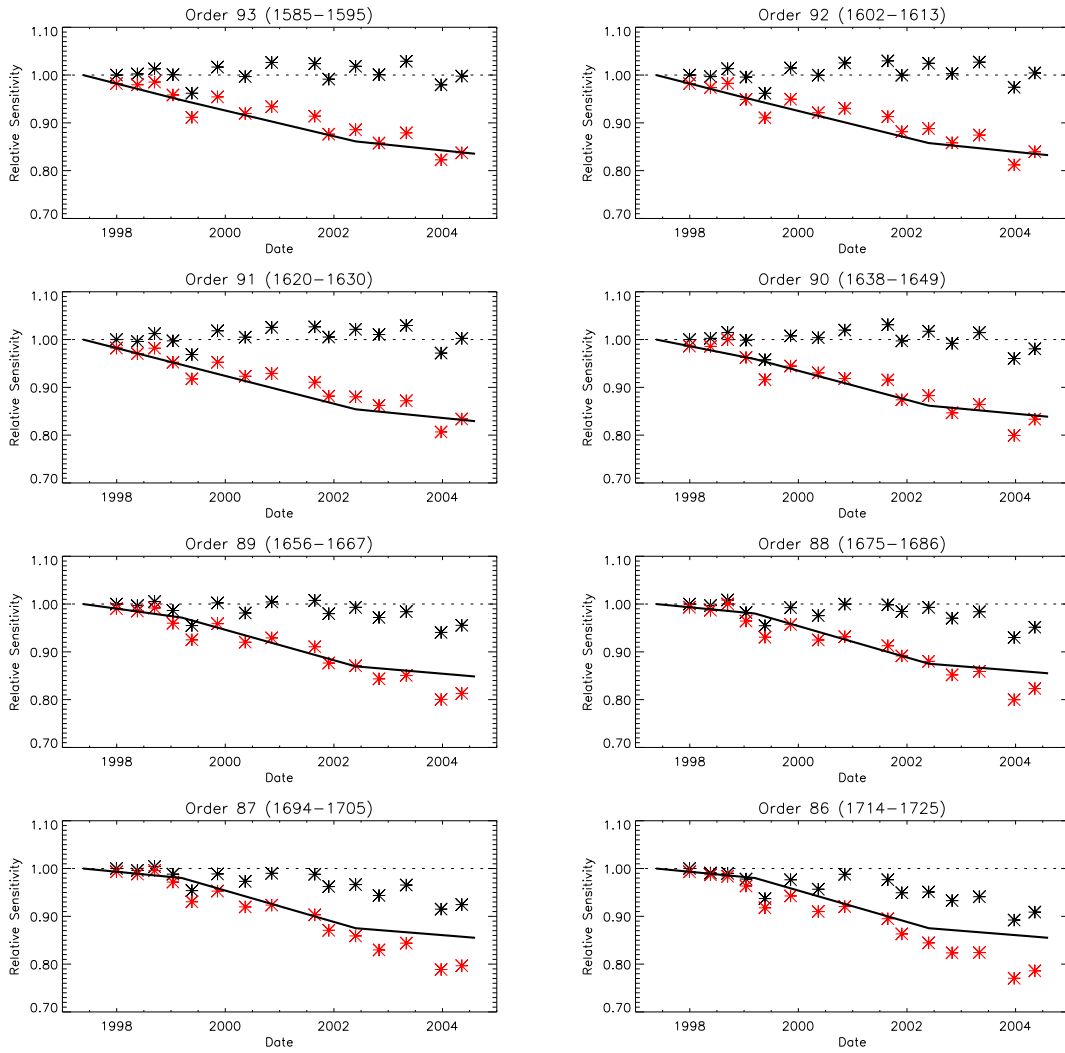


Figure 2. (cont'd)

Instrument Science Report STIS 2011-04

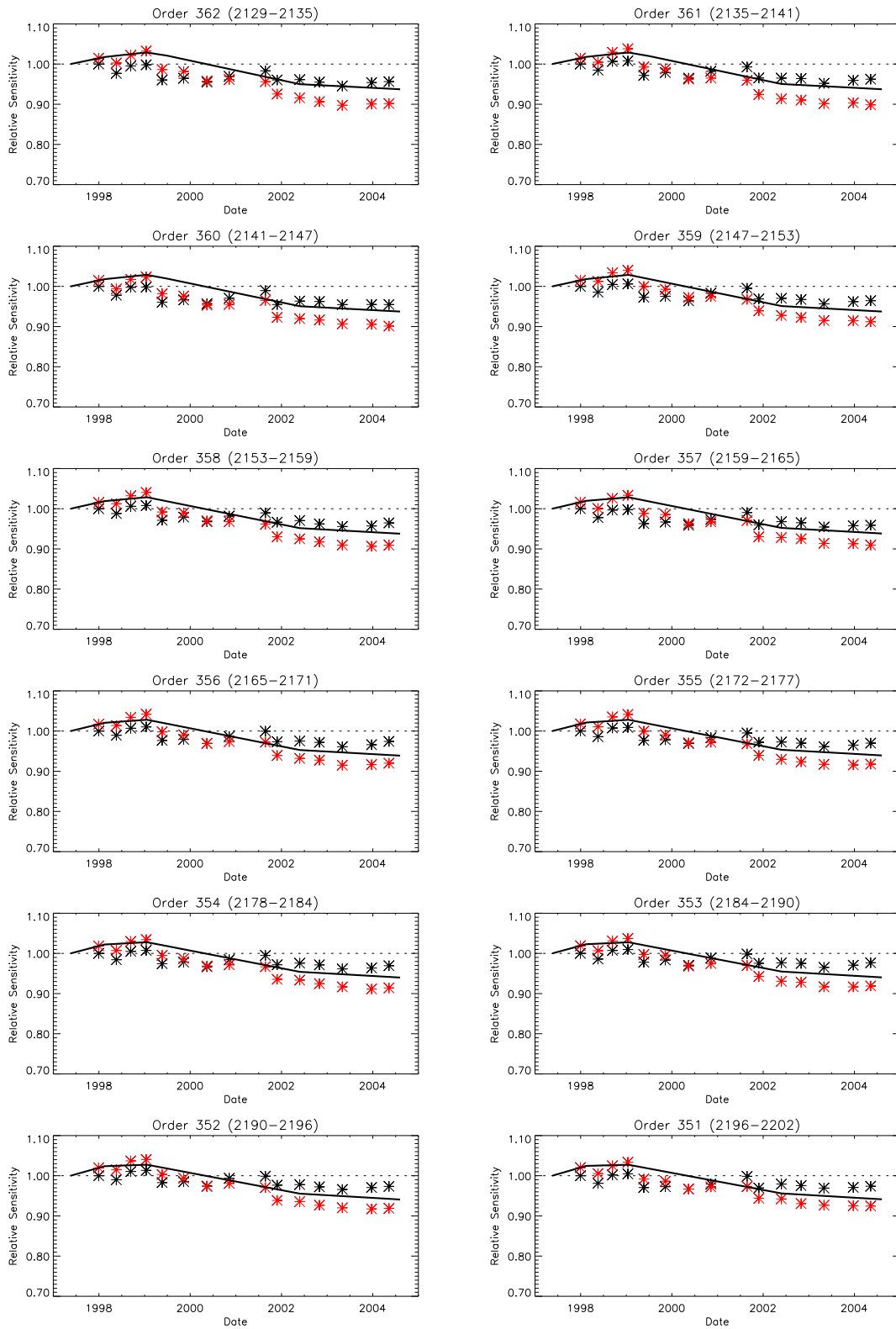


Figure 3. E230H at the central wavelength 2263 Å (~ 2120-2400 Å).

Instrument Science Report STIS 2011-04

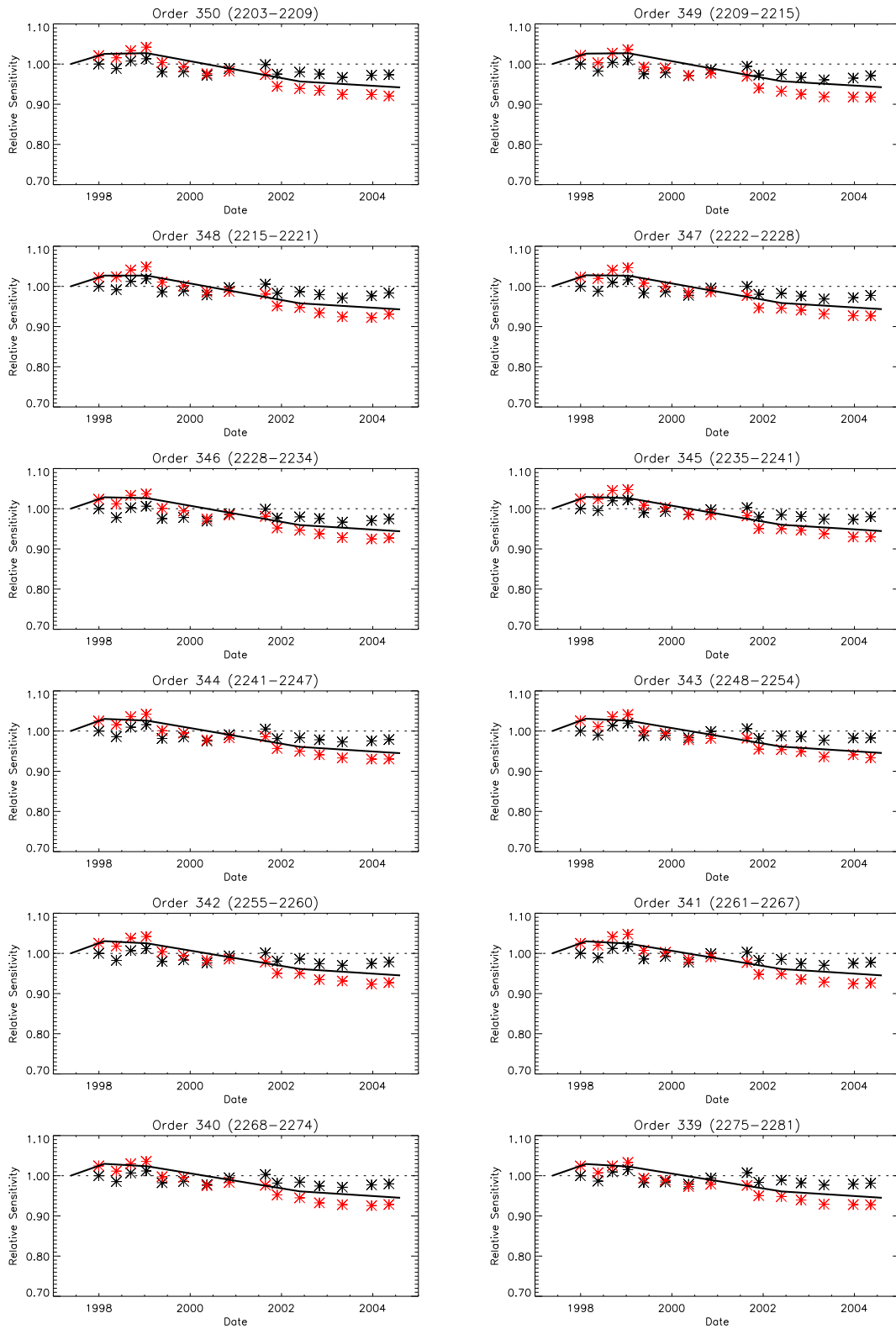


Figure 3. (cont'd)

Instrument Science Report STIS 2011-04

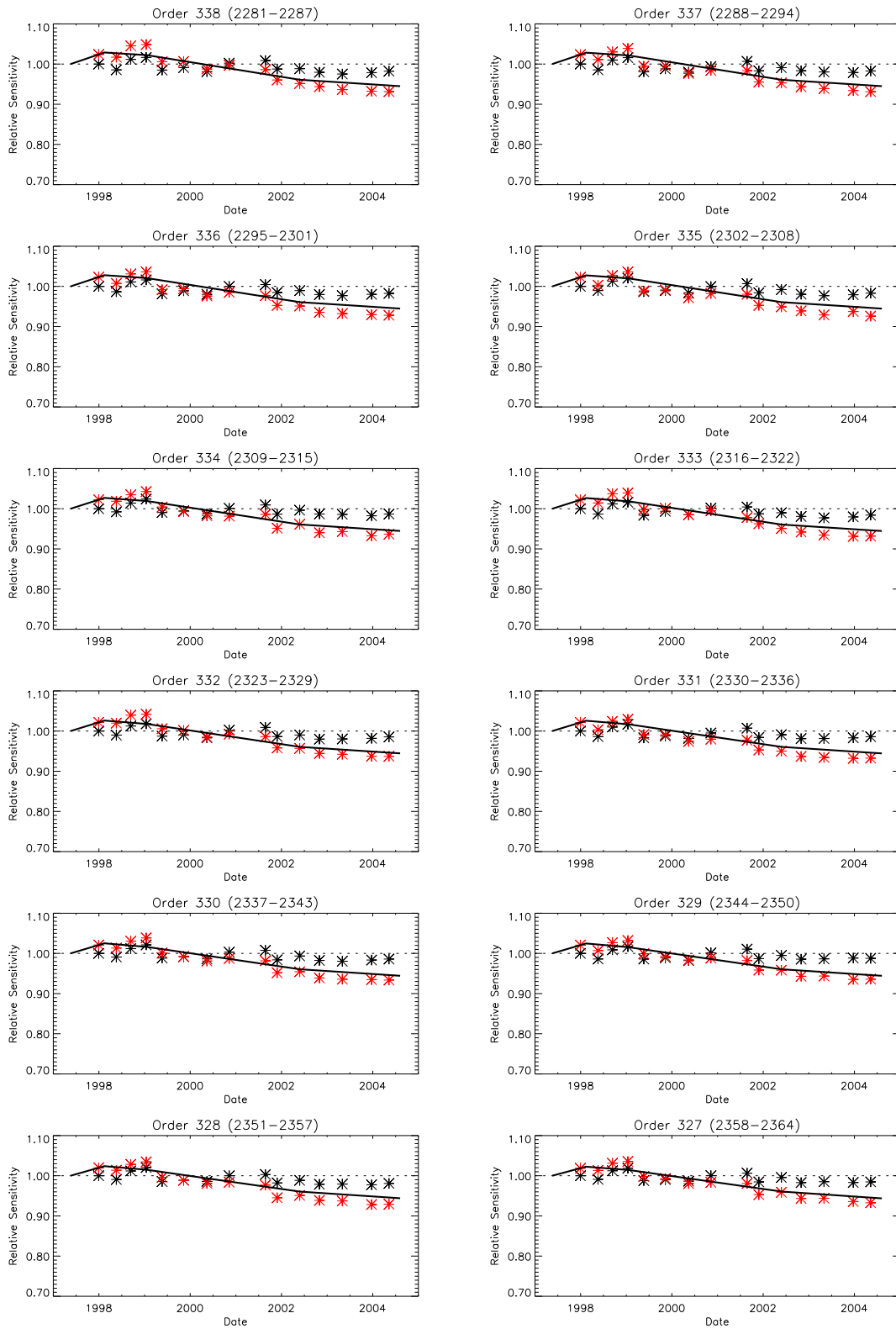


Figure 3. (cont'd)

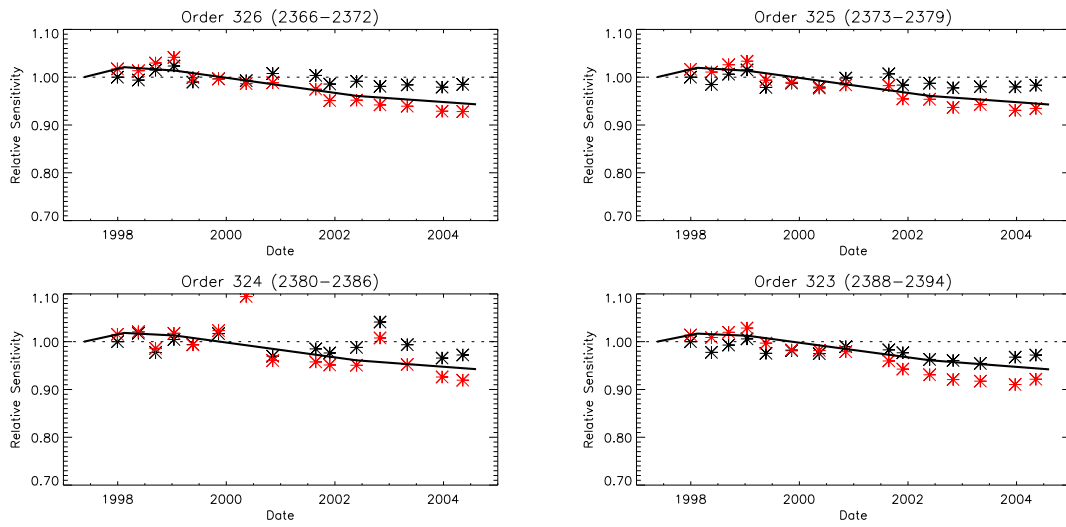


Figure 3. (cont'd)

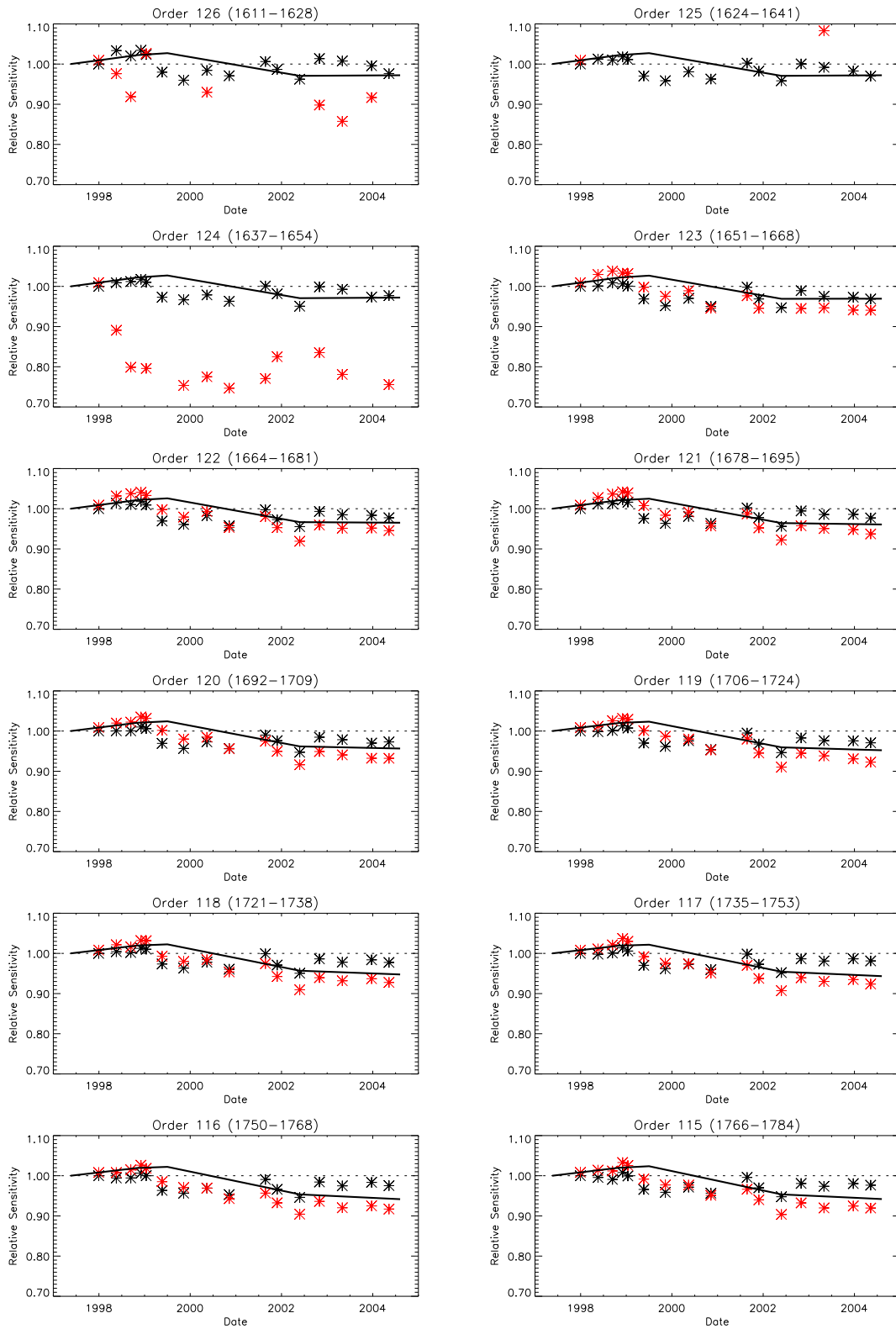


Figure 4. E230M at the central wavelength 1978 Å (~ 1575-2380 Å).

Instrument Science Report STIS 2011-04

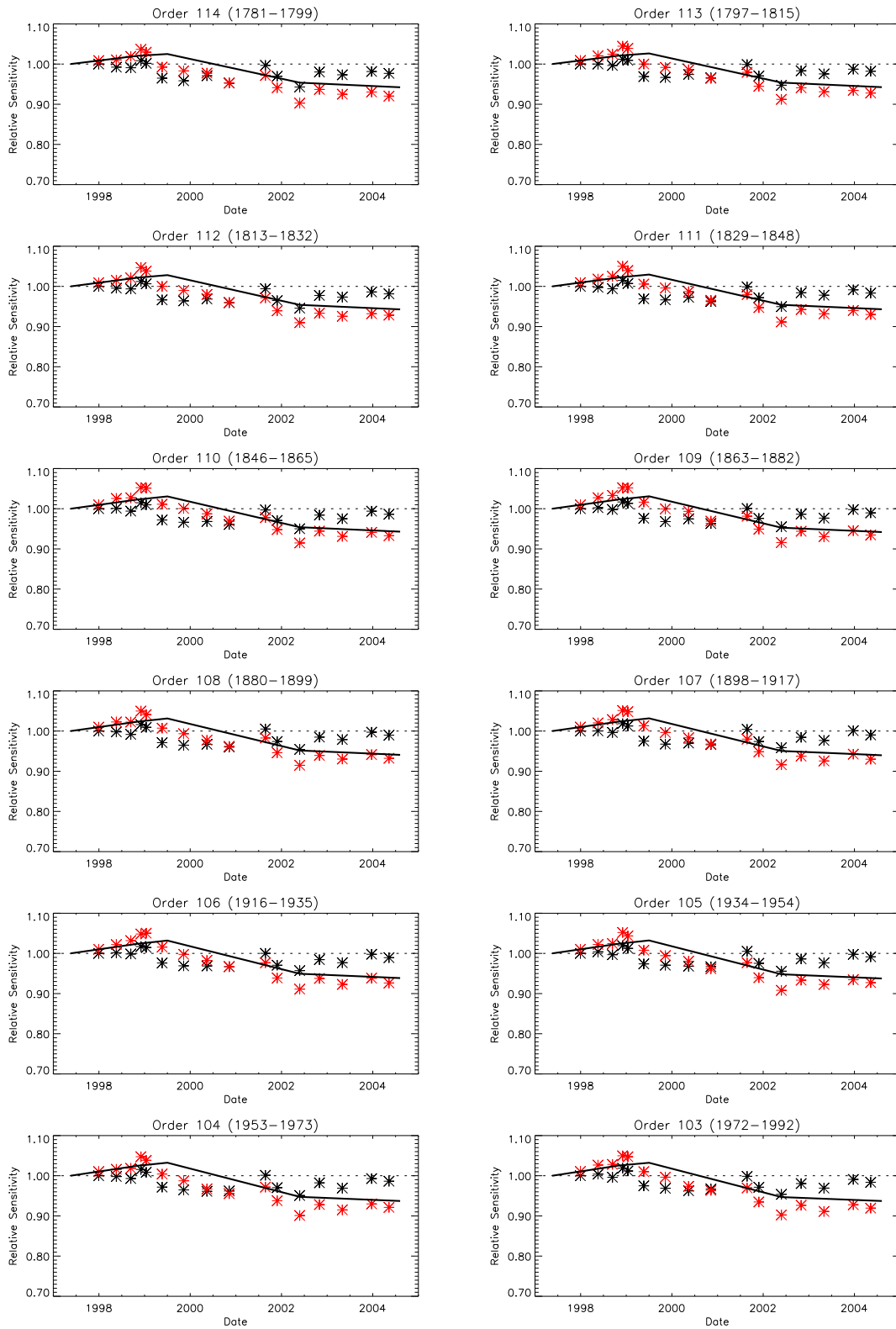


Figure 4. (cont'd)

Instrument Science Report STIS 2011-04

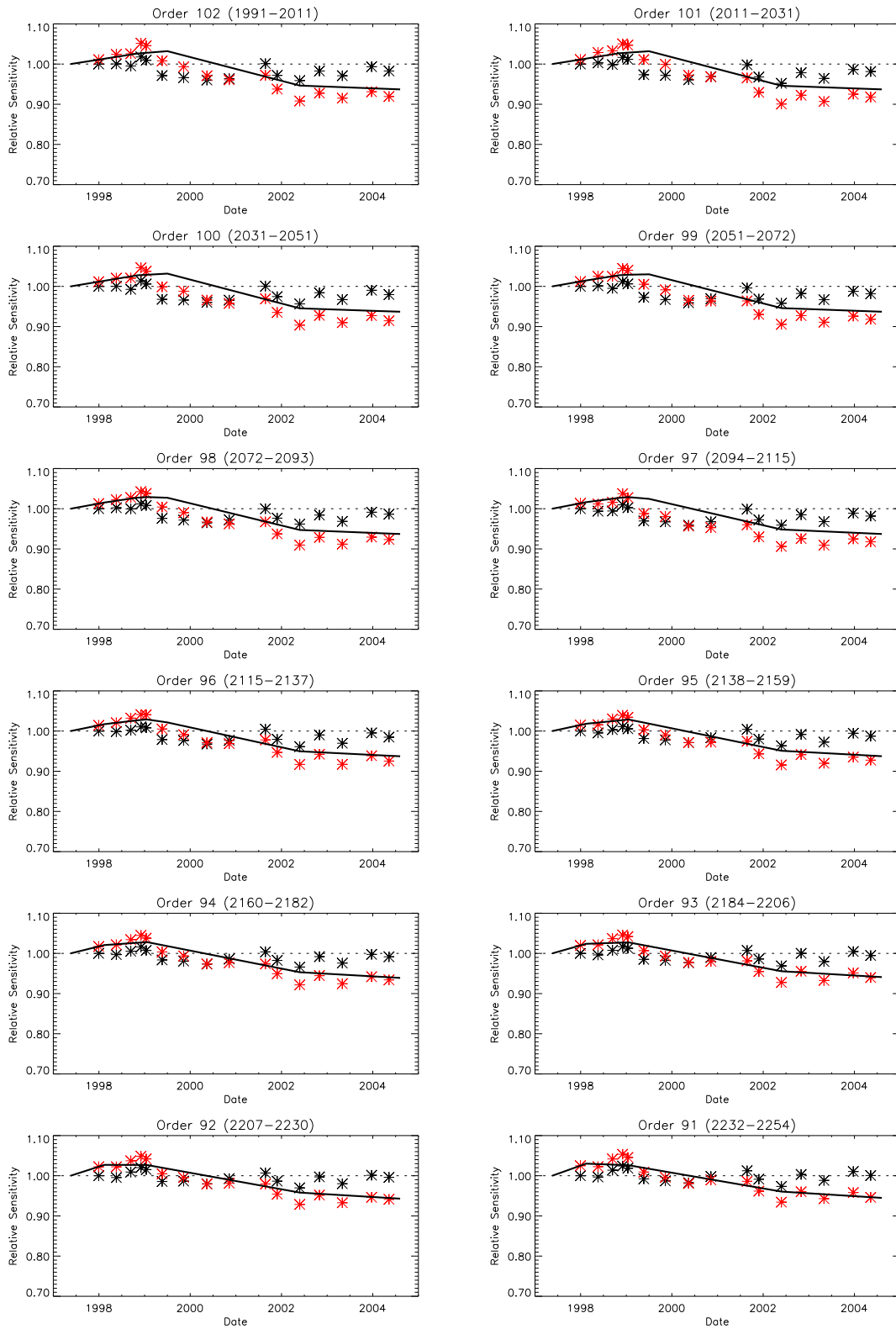


Figure 4. (cont'd)

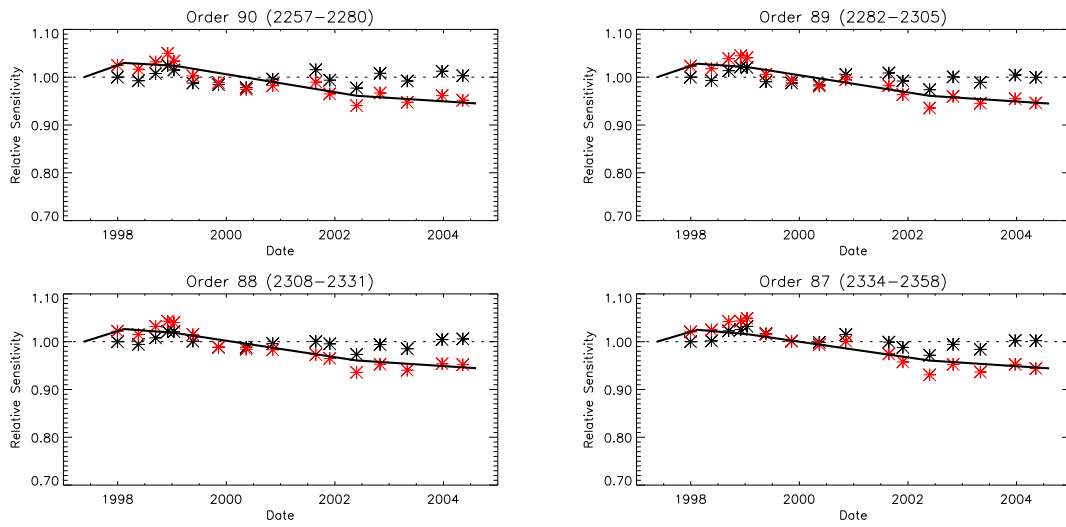


Figure 4. (cont'd)

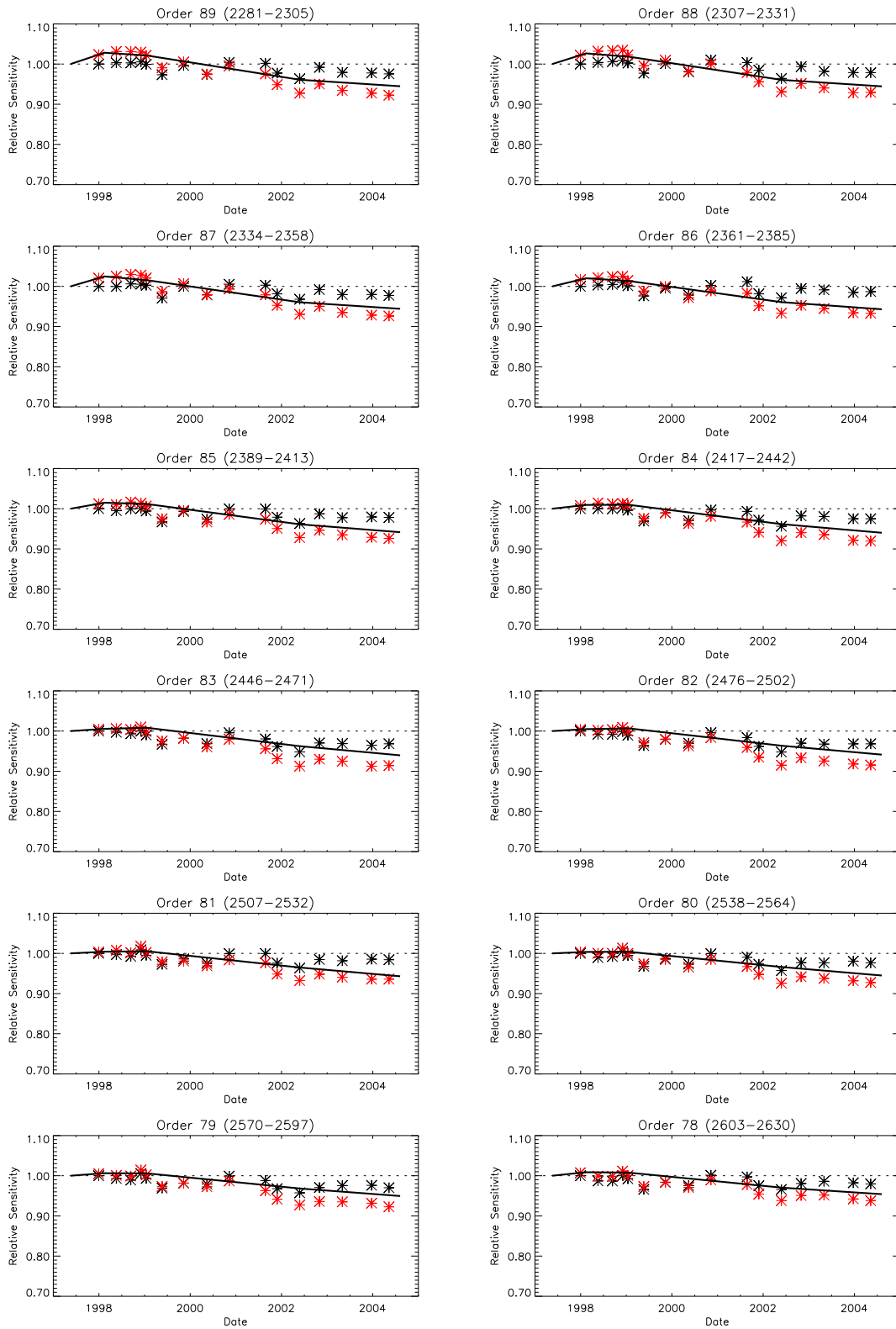


Figure 5. E230M at the central wavelength 2707 Å (~ 2300-3110 Å).

Instrument Science Report STIS 2011-04

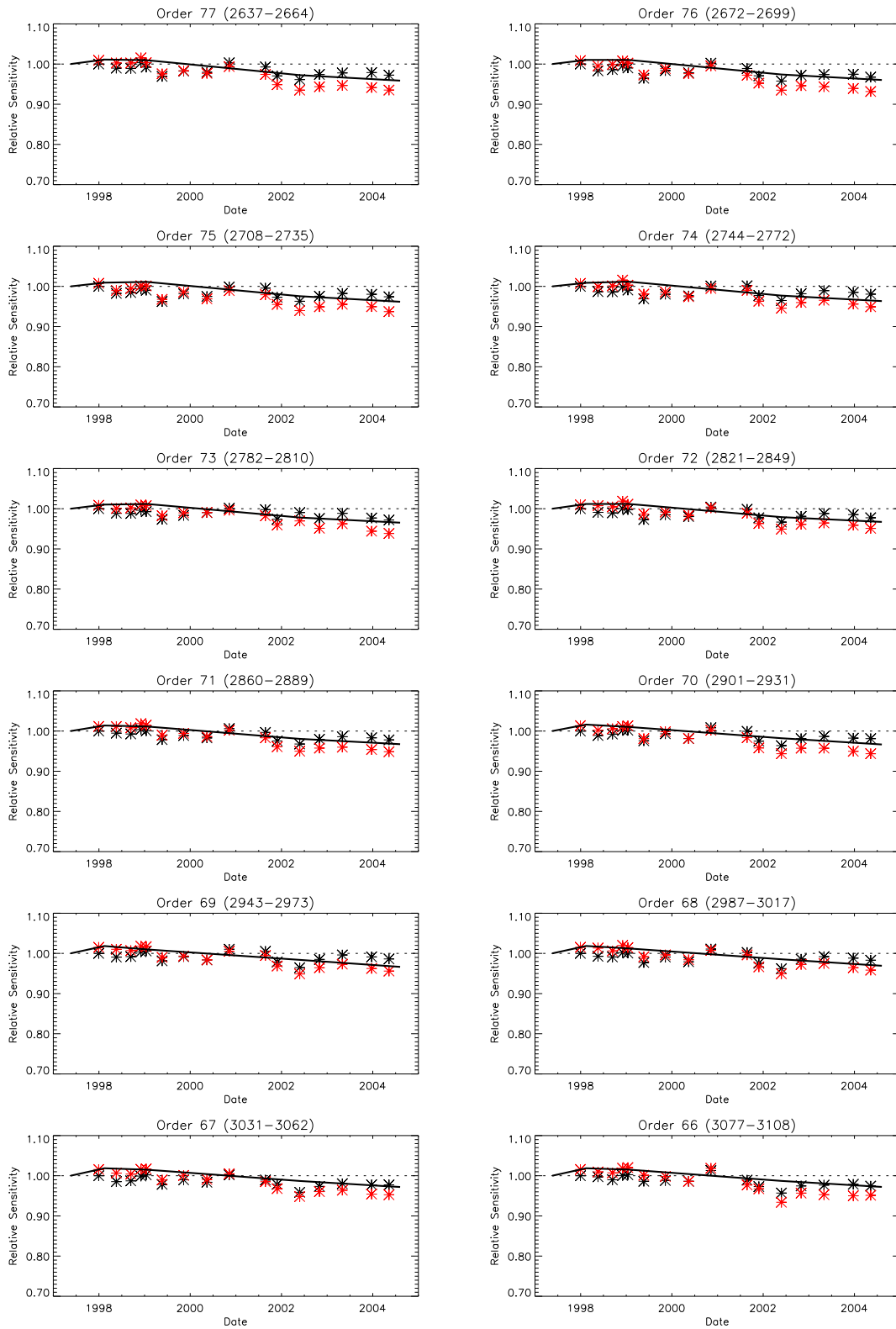


Figure 5. (cont'd)